(t, p) and (p, t) Reactions on Even Ce Isotopes*

T. J. Mulligan†
Department of Physics, Florida State University, Tallahassee, Florida 32036, and Los Alamos Scientific Laboratory, University of California, Los Alamos, New Mexico 87544

and

E. R. Flynn, Ole Hansen, and R. F. Casten
Los Alamos Scientific Laboratory, University of California, Los Alamos, New Mexico 87544

and

R. K. Sheline
Department of Physics, Florida State University, Tallahassee, Florida 32306

(Received 9 August 1971)

The (t,p) reaction on ^{138,140}Ce at 15-MeV incident energy and the (p,t) process on ^{142}Ce at 21.5 MeV have been studied. Differential cross sections were measured between 12 and 66° in 6° intervals and $L=0$ and 2 assignments made. Less extensive data on ^{136,142}Ce(t,p) and ^{140}Ce(p,t) were also acquired and a ^{140}Ce(t,t) angular distribution was obtained at 15 MeV. The strongest $L=0$ and $L=2$ transitions are discussed in relation to the pairing-vibrational model; in particular the 3226-keV state in ^{140}Ce was found to contain about 70% of the (1, 1) two-phonon strength and several candidates for pairing-quadrupole-vibrational states are noted. Anharmonic effects on the energies of pairing-phonon states are considered and a discussion of the observed 3^- strengths is included.

I. INTRODUCTION

The stable Ce isotopes span the $N=82$ shell closure ranging from neutron number $N=78$ (^{136}Ce) to $N=84$ (^{142}Ce). Thus the Ce isotopes provide an important opportunity for a detailed study of the nuclear structure near a magic number and in particular one may study the excitations of the closed-shell nucleus (^{140}Ce) with two-neutron capture as well as with two-neutron pickup reactions.

The main objective of the present experiments was to examine the monopole- and quadrupole-pairing states in nuclei near $N=82$. The pairing-vibrational model[1,2] predicts certain relations between 0^+ states in nuclei near a shell closure, with the ground states above and below the magic nucleus forming two distinct vibrational bands. In the magic nucleus itself ($N=N_0$) an excited two-particle–two-hole 0^+ state is predicted built on the N_0-2 and N_0+2 ground states. Similar excited 0^+ states should also exist away from the shell closure. Such states are built as products of the ground states above and below the shell closure. The model predicts excitation energies as well as two-neutron-transfer cross sections.

Recent extensions of the pairing scheme[1,2,3] include states with spin different from zero and several 2^+ states in ^{138,140,142}Ce are reported here with properties similar to those predicted by the model.

Information on the level structure of the Ce isotopes has been obtained previously from β-decay studies[4-6] and from one-neutron-transfer reactions.[7-10] Results from Ce(p,t) experiments have been reported by Yagi, Aoki, and Sato[11] and by Sherman *et al.*[12]

In the present investigation, the ^{138,140}Ce(t,p) and the ^{142}Ce(p,t) processes were examined in detail. Additional, although less complete, data were obtained on the ^{136,142}Ce(t,p) and the ^{140}Ce(p,t) reactions and triton elastic scattering differential cross sections were measured at 15 MeV for ^{140}Ce.

II. EXPERIMENTAL PROCEDURE AND RESULTS

A. Targets

The ^{140}Ce and ^{142}Ce targets were vacuum evaporated from isotopically enriched CeO_2 while the ^{136}Ce and ^{138}Ce targets were prepared at the Florida State University isotope separator facility to >99% isotopic purity. The isotopic composition of the evaporated targets is given in Table I. The thicknesses were ≈120 μg/cm^2 for the ^{140,142}Ce cases and ≈25 μg/cm^2 for ^{136,138}Ce; carbon backings (≈50 μg/cm^2) were used in all cases.

B. Experimental Procedure

The proton and triton beams were obtained from the Los Alamos Van de Graaff facility and the reactions ^{138,140}Ce(t,p) and ^{142}Ce(p,t) were studied

TABLE I. Composition of CeO_2 material used for vacuum-evaporated target fabrication.

Isotope	^{140}Ce target (at. %)	^{142}Ce target (at. %)
136	<0.02	<0.05
138	0.04	<0.05
140	99.70	7.23
142	0.26	92.77

using a broad-range magnetic spectrograph. The reaction protons and tritons were detected in 50-μm Kodak NTB nuclear track plates which were subsequently scanned under a microscope in 200-μm-wide swaths. The momentum range of the spectrograph together with suitably chosen stopping foils placed in front of the photographic emulsions allowed the simultaneous recording of (t, p) and (t, d) or (p, t) and (p, d) reaction spectra. The details of the various spectrograph exposures are summarized in Table II.

The above mentioned reactions were also examined by using a solid-state counter telescope. Proton, deuteron, and triton spectra were recorded simultaneously so that the ratio $d\sigma$(reaction)/$d\sigma$(elastic scattering) was measured for each reaction under consideration. For the case of ^{142}Ce(t, p) in which only one spectrograph exposure was made, the more extensive counter data were used to substantiate the target mass for the reported proton groups. In all of the (t, p) experiments the incident energies used in the spectrograph and counter-telescope measurements were identical (15.0 MeV) within the practical limits of the accelerator. However, for the (p, t) case the counter data, due to accelerator conditions, had to be taken at 20 MeV rather than at 21.5 MeV as used in the spectrograph exposures.

The ^{140}Ce(t, t) reaction was measured as a separate counter experiment at an incident energy of 15 MeV. The triton angular distribution was observed from 12 to 120° in 3° increments.

C. Data Analysis and Results

1. *Triton Elastic Scattering*

The ^{140}Ce(t, t) data were analyzed using the optical-model search code of Perey[13] which has Woods-Saxon shapes for the real and imaginary potentials. In accordance with the triton-scattering study of Flynn *et al.*,[14] the radial parameter of the real well was fixed at $r_r = 1.16$ fm and the charge radius was set at 1.25 fm. The real and imaginary depths and diffusenesses as well as the imaginary radius were varied to obtain the best fit to the measured values. No spin-orbit term was included. A normalization factor was chosen by considering the points forward of 27°, since at these forward angles the cross section is largely due to Rutherford scattering and is quite insensitive to the choice of optical-model parameters. The final set of parameters obtained for this experiment are presented in Table III together with the average-geometry parameters of Ref. 14. The fit to the data using the best-fit values is shown in Fig. 1. The fact that the best-fit parameters are so close to the average-geometry set is reassuring, since the latter set is used for distorted-wave Born-approximation (DWBA) calculations in order to permit the use of an absolute normalization factor as discussed in Sec. III.

2. *Reaction Data*

The data from the ^{140}Ce(t, p) experiment are summarized in Table IV. This table presents the excitation energies, the maximum cross sections, and the angular-momentum transfers observed in this reaction. In addition, previously established ^{142}Ce levels with their J^π are shown. Figure 2 shows a typical spectrum from this reaction, while Fig. 3 shows the differential cross sections for this reaction. The ^{142}Ce spectrum was analyzed up

TABLE II. The spectrograph exposures.

Reaction	Bombarding energy (MeV)	Angular range θ_{min}	Angular range θ_{max}	$\Delta\theta$	Exposure [a] (μC)	Energy resolution (keV; full width at half maximum)
^{138}Ce(t, p)	15	12	66	6	8000	23
^{140}Ce(t, p)	15	15	72	6	8000	18
^{142}Ce(t, p)	15	30			6977	19
^{142}Ce(p, t)	21.5	12	66	6	6000	16
^{140}Ce(p, t)						

[a] The exposures sometimes varied from angle to angle. The value given is typical for the experiment under consideration.

TABLE III. Triton optical-model parameters for $^{140}Ce(t,t)$ elastic scattering at 15 MeV.

	V (MeV)	r_r (fm)	a_r (fm)	W (MeV)	r_i (fm)	a_i (fm)	r_c (fm)	χ^2
Best fit	166.41	1.16	0.745	15.165	1.452	0.864	1.25	1.02
Average geometry	166.7	1.16	0.752	15.66	1.498	0.817	1.25	6.38

to ≈4 MeV of excitation and the absolute-cross-section scale for this reaction was established from the observed ratio of $d\sigma[^{140}Ce(t,p)]/d\sigma[^{140}Ce(t,t)]$ to an accuracy of better than ±15%. The $^{140}Ce(t,p)$ Q value of 4112 ± 5 keV was measured relative to the ^{12}C and $^{16}O(t,p)$ ground-state Q values and agrees well with the value of 4108 ± 4 keV obtained from mass data.[15]

The $^{138}Ce(t,p)$ and $^{142}Ce(p,t)$ results are presented in Table V. Typical spectra are shown in Figs. 4 and 5, while the angular distributions are shown in Figs. 6 and 7. The spectra were analyzed in detail up to excitation energies of 4.2 and 4.8 MeV for the (t,p) and (p,t) cases, respectively; no strong transitions leading to states in ^{140}Ce were observed above these limits. Absolute cross sections for the $^{138}Ce(t,p)$ reaction were established in the same way as used for $^{140}Ce(t,p)$. The $^{138}Ce(t,p)$ ground-state Q value of 8184 ± 15 keV agrees well with the mass Q value of 8167 ± 19 keV.[16]

The ^{142}Ce target contained enough ^{140}Ce to allow the identification of the ^{138}Ce ground- and first-excited states in the (p,t) study. The absolute cross sections for the $^{140,142}Ce(p,t)$ reactions were measured at 20 MeV by the same method used for the (t,p) cases. The 21.5-MeV spectrograph data were connected to the 20-MeV counter measurements by distorted-wave (DW) calculations which show that $d\sigma(21.5\ \text{MeV}) = 0.9\,d\sigma(20\ \text{MeV})$ for the

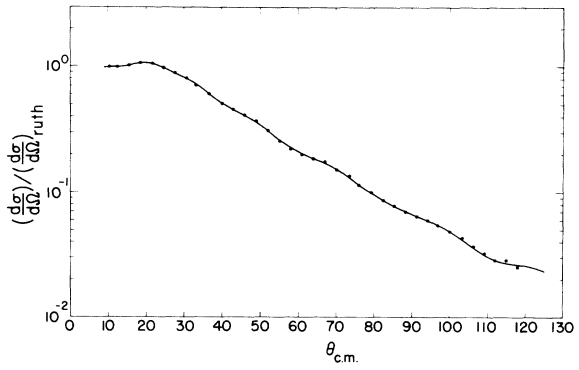

FIG. 1. Cross-section angular distribution for the $^{140}Ce(t,t)$ experiment at 15 MeV. The dots represent data points while the solid curve shows the optical-model fit using the "best-fit" parameters of Table III.

TABLE IV. Results of the $^{140}Ce(t,p)^{142}Ce$ reaction.

Proton group No.	Energy (keV)	$(mb/sr)_{max}$	L	Decay data (Ref. 5)	J^π
1	0	0.340	0	0	0^+
2	642 ± 3	0.600	2	641.2	2^+
3	1220 ± 4	0.431		1219.3	
				1536.1	2^+
4	1652 ± 3	0.162	3	1652.6	3^-
5	1742 ± 3	0.133			
6	2005 ± 3	0.240	2	2004.2	2^+
7	2043 ± 3	0.040			
8	2114 ± 4	0.045			
9	2125 ± 3	0.155			
				2181.4	
10	2188 ± 3	0.050		2187.2	
11	2279 ± 3	0.046			
12	2367 ± 3	0.025			
				2364.4	
				2397.7	1^-
13	2542 ± 3	0.044		2542.7	
14	2604 ± 4	0.102			
				2666.8	
15	2701 ± 5	0.092		2696.3	
16	2735 ± 5	0.113		2741.5	
17	2775 ± 5	0.009			
18	2810 ± 4	0.038			
19	2861 ± 4	0.102			
20	2922 ± 4	0.096			
21	2986 ± 5	0.026			
22	2999 ± 5	0.022			
23	3067 ± 4	0.026			
24	3165 ± 5	0.029			
25	3228 ± 4	0.075			
				3420.4	
26	3436 ± 4	0.021			
				3459.3	$(2^+, 1^-)$
				3470.0	
27	3614 ± 4	0.034		3612.1	
				3613.0	
				3632.7	
				3675.4	
				3717.0	
				3719.1	
28	3732 ± 4	0.076		3746.3	

ground-state transition. The accuracy of the (p,t) cross-section scale is believed to be ±20%.

In the ^{136}Ce(t,p) case, only counter-telescope data of the ground-state cross section were measured. In the ^{142}Ce(t,p) reaction one spectrograph spectrum was taken which gave a ground-state Q value of 3582 ± 15 keV as compared to the mass Q value of 3579 ± 9 keV.[15]

III. DW ANALYSIS

Assuming that the (t,p) and (p,t) reactions proceed by a simple direct mechanism, the DW code TWOPAR by Bayman and Kallio[17] was used to calculate the angular distributions of orbital angular momentum transfers from $L=0$ to $L=6$. These calculations were used for both L assignments and analysis of cross-section magnitudes. The calculations followed the prescription of Flynn and Hansen[18] and the normalization factor of 310 suggested in this reference was used when comparing the calculated cross sections to the data. The optical-model parameters used in the calculations are shown in Table VI. The triton parameters are those of Ref. 14 as mentioned in Sec. II C 1, while the proton parameters were derived using the prescription given by Perey in Ref. 13, Eq. (2).

Since the shape for a given L transfer was found to be insensitive to configuration mixing, the assignment of L values was based on calculations using pure-configuration form factors. For the case of $L=0$ and $L=2$ transitions the angular-distribution shapes are distinctive and fits to the data are good. No known 1^- levels were excited so that the assignment of $L=1$ transitions is uncertain. A similar situation holds true for higher L transi-

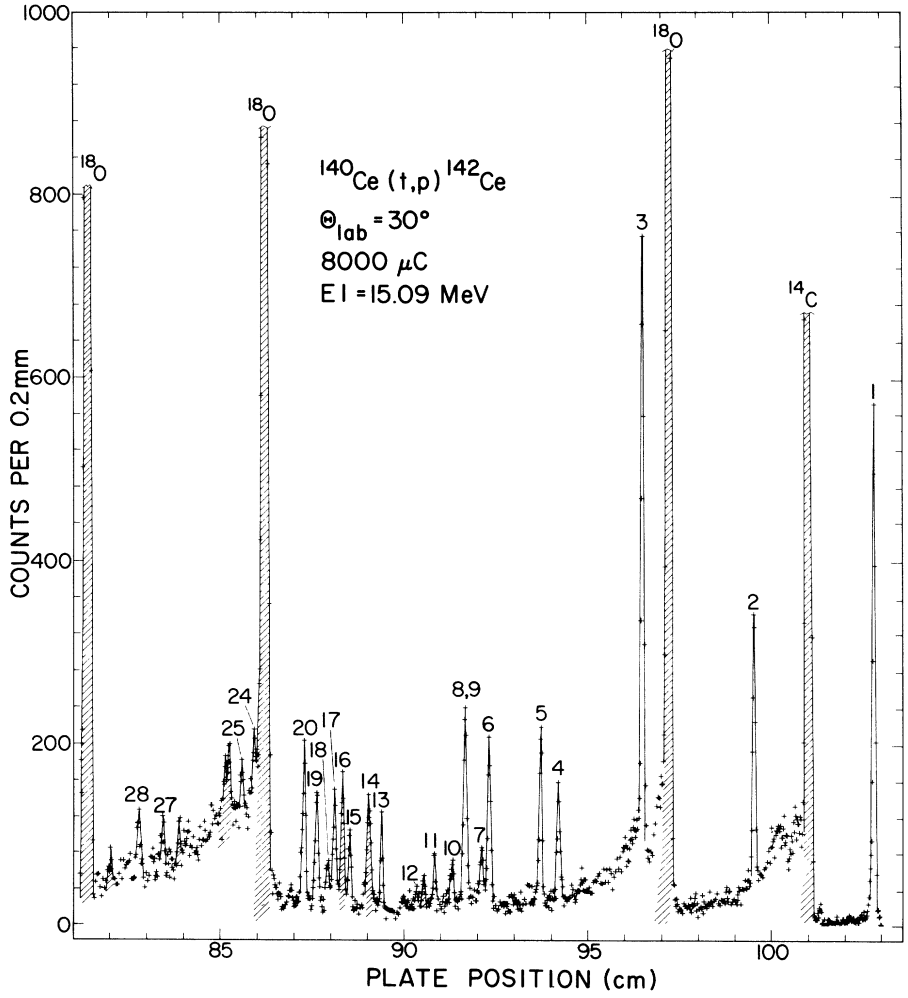

FIG. 2. Sample spectrum from the ^{140}Ce(t,p) reaction. The numbers above the peaks refer to the proton group numbers of Table IV. The major impurity peaks are cross-hatched while those due to C and O are labeled by the residual nuclei.

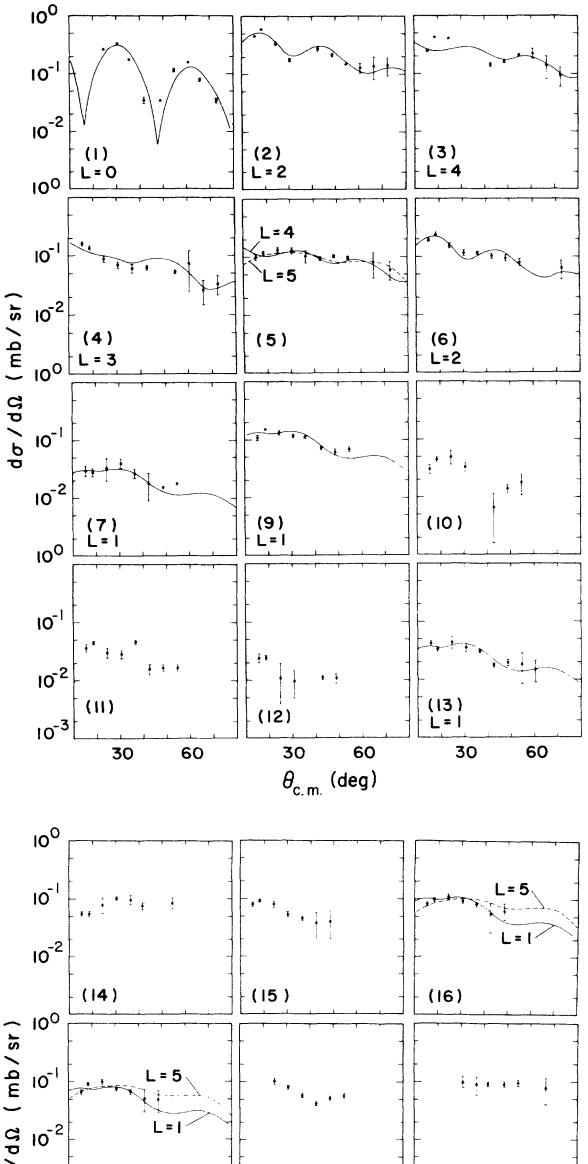

FIG. 3. Cross-section angular distributions for the ^{140}Ce(t,p) reaction. The numbers in parentheses refer to the proton group numbers of Table IV. The solid lines are DWBA fits which have been normalized to the data and represent the L transfer labeled for each case. The DWBA curves are shown only for comparison to the data and do not imply an assignment of L value. All ^{140}Ce(t,p) L value assignments are shown in Table IV.

tions with the exception of $L=3$. There are known 3^- states in ^{140}Ce and ^{142}Ce and from Figs. 3, 6, and 7 it can be seen that, although no L assignment is possible in these 3^- cases based on our data, the angular distributions are consistent with an $L=3$ shape. The shapes for $L>3$ transitions are generally flat and uncharacteristic, especially at low Q values, making reliable L assignments impossible.

IV. DISCUSSION

A. Comparison to Other Data

Recent high-resolution decay-scheme work[4,5] on levels in ^{140}Ce and ^{142}Ce has yielded accurate energy levels and several spin assignments. Of the 24 ^{140}Ce levels populated by the (t,p) and (p,t) reactions four are also observed in β decay. The excitation energies of the present work agree well with the more accurate numbers from the decay data and no discrepancies of spin assignments are observed.

In the ^{142}Ce case, nine of the 28 levels populated by ^{140}Ce(t,p) are also observed in the decay scheme, and the spin and parity assignments from the decay work are generally consistent with the present results. The fact that 16 out of 18 levels in ^{140}Ce populated by the $(^3\text{He},d)$ and $(d,^3\text{He})$ proton-transfer reactions[10] are also observed in the decay work demonstrates that many of the states are proton excitations and hence, should not be strongly excited in the present neutron-transfer reactions.

B. 3^- States

The 2469-keV level in ^{140}Ce and the 1652-keV level in ^{142}Ce are both known to have $J^\pi=3^-$ and to be of collective nature.[19] These states are populated in the (t,p) reactions with maximum cross sections of 0.033 and 0.16 mb/sr, respectively, while the (p,t) reaction on ^{142}Ce excites the ^{140}Ce 3^- state with a maximum value of 0.04 mb/sr. The outstanding feature is the factor of five increase in (t,p) cross section in going from ^{140}Ce to ^{142}Ce.

A similar trend is observed in the Ca and Cr (t,p) data[20,21] where it can be explained, at least qualitatively, by considering the microscopic composition of the 3^- levels. Below the $N=28$ shell closure in Ca and Cr the important 3^- components are blocked in the (t,p) reaction while above $N=28$ the availability of the $p_{3/2}g_{9/2}$ configuration gives rise to the increased cross section.

The neutron part of the ^{140}Ce 3^- state should have particle-hole character with the holes coming from the occupied $d_{3/2}$ and $s_{1/2}$ orbits and the particles being in the unoccupied $f_{7/2}$, $p_{1/2}$, $f_{5/2}$ orbits. Due to configuration mixing most of the possible particle-hole configurations needed to excite the 3^-

state in ^{140}Ce via a two-neutron transfer are available in the $^{138, 142}$Ce ground states and, in analogy with the situation, in ^{208}Pb the 3^- transition was expected to proceed strongly.[22] DW calculations using pure-configuration form factors consisting of $s_{1/2}$ or $d_{3/2}$ holes and $f_{7/2}$, $f_{5/2}$, or $p_{3/2}$ particles predict cross sections equal to or larger than the experimentally observed number for each possible 3^- particle-hole configuration. It is not understood why the Ce situation differs from the Pb case.

The case of the ^{142}Ce 3^- state is somewhat different because two different types of configurations are now possible for 3^- construction. One type is the ^{140}Ce 3^- state coupled with the $J=0$ pairing phonon; the other is the two-particle 3^- state composed principally of the configuration $(f_{7/2}, i_{13/2})$ coupled to the ^{140}Ce ground state. The latter type is easily excited in the (t, p) reaction while the first type is available only through ground-state correlations in ^{140}Ce or through a second-order (t, p) process. The pronounced drop in energy of the octopole level is probably also due to the existence of this two-particle 3^- state as has been shown in lead.[23] In fact, the $(f_{7/2}, i_{13/2})$ configuration can account for 60% of the observed cross section to the ^{142}Ce 3^- state.

An explanation of these results must await a detailed analysis of the microscopic structure of both 3^- levels and the possible effects of two-step processes which have been shown to be important for low-lying collective 3^- states.[23]

TABLE V. Levels in ^{140}Ce populated in the (t, p) and (p, t) reactions.

	^{138}Ce(t, p)			^{140}Ce		^{142}Ce(p, t)		
Level	Energy			Decay data		Energy		
No.	(keV)	L	$(\mathrm{mb/sr})_{max}$	E	J^π	(keV)	L	$(\mathrm{mb/sr})_{max}$
1	0	0	0.210	0	0^+	0	0	0.765
2	1601 ± 4	2	0.034	1596.6	2^+	1600 ± 6	2	0.167
3	1905 ± 4		0.014	1903.5	0^+	1906 ± 6	0	0.088
4				2083.6	4^+			
5				2108.2	$(6)^+$			
6				2348.4	2^+			
7				2350.2	$(5)^-$			
8				2412.4	3^+			
9	2469 ± 5		0.033	2464.4	3^-	2468 ± 8		0.038
10				2481.3	$(4)^+$			
11				2516.1	$(3, 4)^+$			
12				2521.8	2^+			
13				2547.5	$(1, 2)^+$			
14				2899.7	$(1, 2)^+$			
15	3024 ± 3		0.019			3020 ± 8		0.031
16				3118.3	$(1, 2)^+$			
17	3125 ± 5		0.009					
18	3226 ± 2	0	0.212			3223 ± 5	0	0.526
19				3319.7	$(1, 2)^+$			
20	3331 ± 6		~0.040					
21						3540 ± 7		0.033
22	3551 ± 3	(2)	0.031					
23	3653 ± 3		0.032			3654 ± 7	2	0.066
24	3708 ± 3		0.052			3709 ± 7		~0.030
25	3729 ± 2	2	0.230			3731 ± 7	2	0.320
26	3746 ± 2		(0.06)			3744 ± 7		(0.08)
27	3787 ± 2		0.025					
28	3909 ± 3		0.014					
29						3965 ± 8	2	0.044
30	4119 ± 4		0.022			4123 ± 8	2	0.042
31	4170 ± 2		0.032					
32						4188 ± 8	2	0.030
33	4230 ± 3		0.008					
34						4242 ± 8		0.040
35						4301 ± 9		0.024
36						4429 ± 9		0.030
37						4831 ± 8	2	0.140

C. Monopole Pairing States

A macroscopic description of the pairing-vibration model has been presented by Bohr,[1] by Nathan,[2] and by Hansen.[24] In this model the correlated ground state of a closed- or doubly-closed-shell nucleus of mass A_0 is considered to be the basis or vacuum state $|0\rangle$. The ground state of the nucleus with two more neutrons (mass A_0+2) is thought of as a one-phonon state built on $|0\rangle$ and is represented in this model as $B_>^\dagger|0\rangle$. The creation operator $B_>^\dagger$ consists mainly of a coherent sum over two-particle creation operators for neutrons in orbits above the closed shell. The remaining part of $B_>^\dagger$ is made up of a coherent sum over two-hole destruction operators for levels below the closed shell. Likewise, the ground state of the A_0-2 nucleus with two neutrons less than A_0 is represented by $B_<^\dagger|0\rangle$. Here the $B_<^\dagger$ operator is composed mainly of two-hole creation operators for levels below the closed shell with the remaining part being two-particle destruction operators for states above the closed shell.

This scheme may be extended so that the A_0+4 ground state is described as a two-phonon state $B_>^\dagger B_>^\dagger|0\rangle$ while the A_0-4 ground state is represented by $B_<^\dagger B_<^\dagger|0\rangle$. The state $B_>^\dagger B_<^\dagger|0\rangle$ is then expected to occur as an excited level in the nucleus A_0 (the closed-shell nucleus). This state, which is referred to as the (1, 1) monopole-pairing vibration (see caption of Fig. 8 for explanation of nomenclature) can be reached from the nucleus A_0+2 by addition of a $B_<^\dagger$ phonon [e.g., via the (p, t) reaction] while in going from A_0-2 one must add a $B_>^\dagger$ pho-

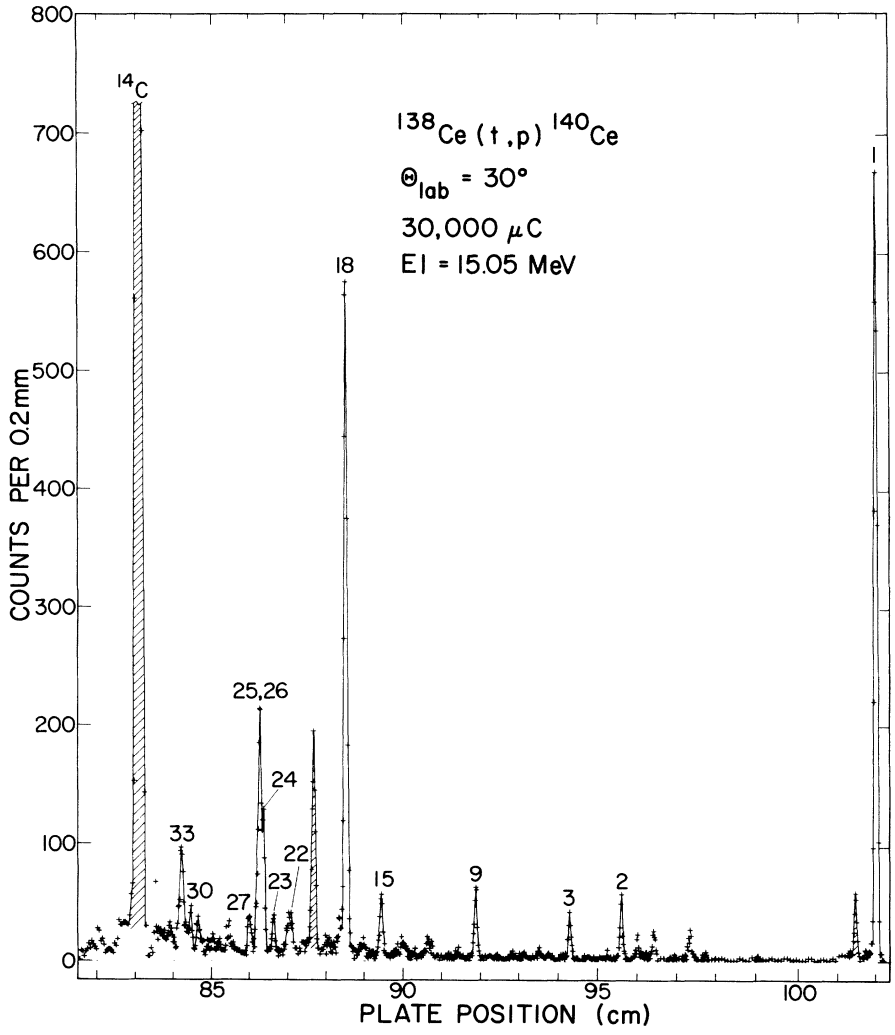

FIG. 4. Sample spectrum from the ^{138}Ce(t, p) reaction. The numbers above the peaks refer to the level numbers of Table V. The major impurity peaks are cross-hatched and the ^{12}C$(t, p)^{14}$C(g.s.) group is labeled.

non [e.g., via the (t,p) reaction]. Thus the (t,p) and (p,t) cross sections to this state have simple relations to the $A_0 \rightarrow A_0+2$ and the $A_0 \rightarrow A_0-2$ ground-state transitions, respectively. The energy and two-neutron transition-strength relations of this harmonic-pairing-vibration model are shown in Fig. 8.

Using the above model for an interpretation of the $L=0$ transitions in the Ce isotopes, the ^{140}Ce ground state is assigned as the vacuum state, the ^{142}Ce ground state as the (0, 1) pair-addition one-phonon state, and the ^{138}Ce ground state as the pair-removal (1, 0) one-phonon state. The fact that only one $L=0$ transition is observed in the ^{140}Ce(t,p) spectrum (the ground-state transition) indicates that this state must be coherently mixed, since in the pure shell model the ground state would be $(2f_{7/2})^2$ with a $(3p_{3/2})^2$ 0^+ level at ~1.5 MeV with about twice the cross section. The (d,t) data,[7] from which the estimate of the $(3p_{3/2})^2$ energy was taken, also demonstrate considerable mixing in the ^{142}Ce ground state. The observed ^{140}Ce(t,p)-^{142}Ce(g.s.) cross section is ~2 times the expected $(2f_{7/2})^2$ value while it is ~0.9 times the cross section using the pairing wave function of Fulmer, McCarthy, and Cohen.[7]

In the pair-removal case, the ^{140}Ce$(p,t)^{138}$Ce and in the inverse reaction, the measured cross sections are compared with the expected $(2d_{3/2})^2$ configuration value. There is no one-neutron-transfer data available on ^{138}Ce and the present (p,t) data do not indicate whether excited 0^+ states are populated in ^{138}Ce. The enhancements over pure configurations found in the present work are in agreement with the findings near other closed shells[18, 23] and indicate a situation where pairing mixing is

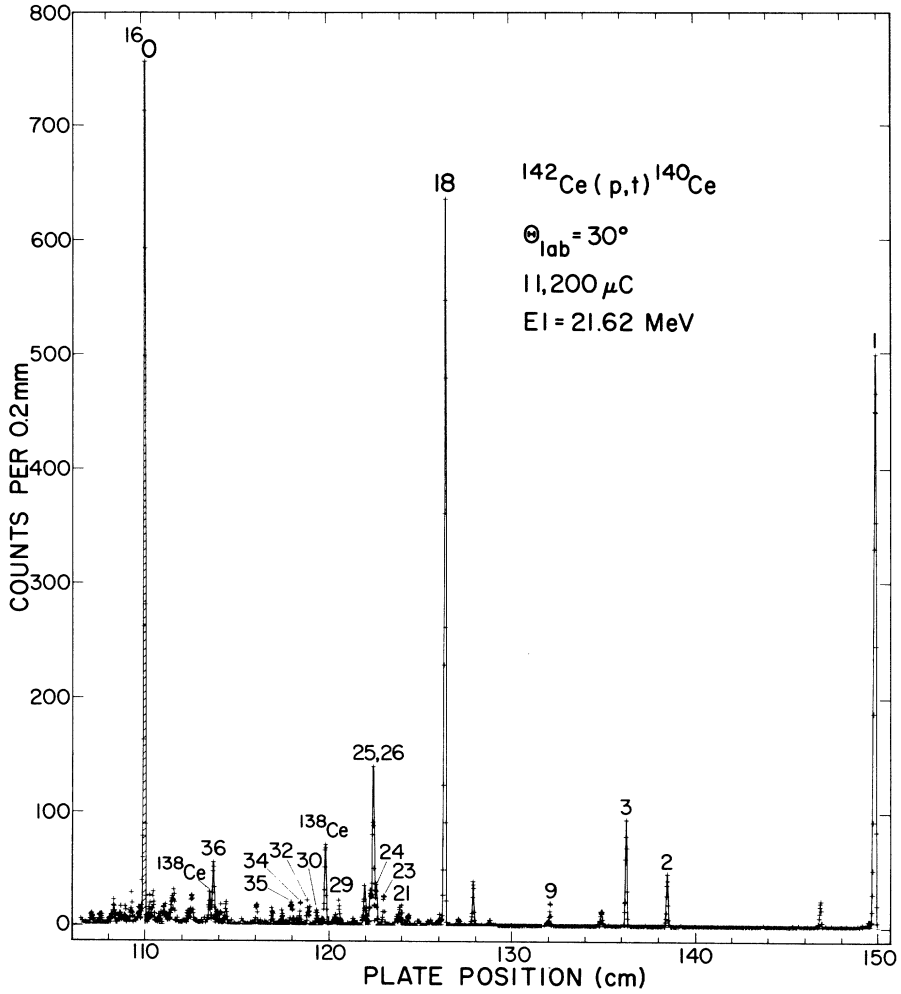

FIG. 5. Sample spectrum from the ^{142}Ce(p,t) reaction. The numbers above the peaks refer to the level numbers of Table V. The ^{18}O$(p,t)^{16}$O(g.s.) group is labeled and cross-hatched.

present but the superconducting state has not been reached.

The ^{140}Ce 0^+ state at 3.226 MeV has approximately the properties expected for the (1, 1) two-phonon-pairing vibration. It is the only strongly populated excited 0^+ state observed in ^{140}Ce in the present work. Although its energy is ~850 keV lower than predicted in the harmonic approximation (see Fig. 9), the (t, p) cross section is ~60% of the ^{140}Ce$(t, p)^{142}$Ce(g.s.) strength (100% is expected in the harmonic limit) and the (p, t) cross section is also 60% of the ^{140}Ce$(p, t)^{138}$Ce(g.s.) val-

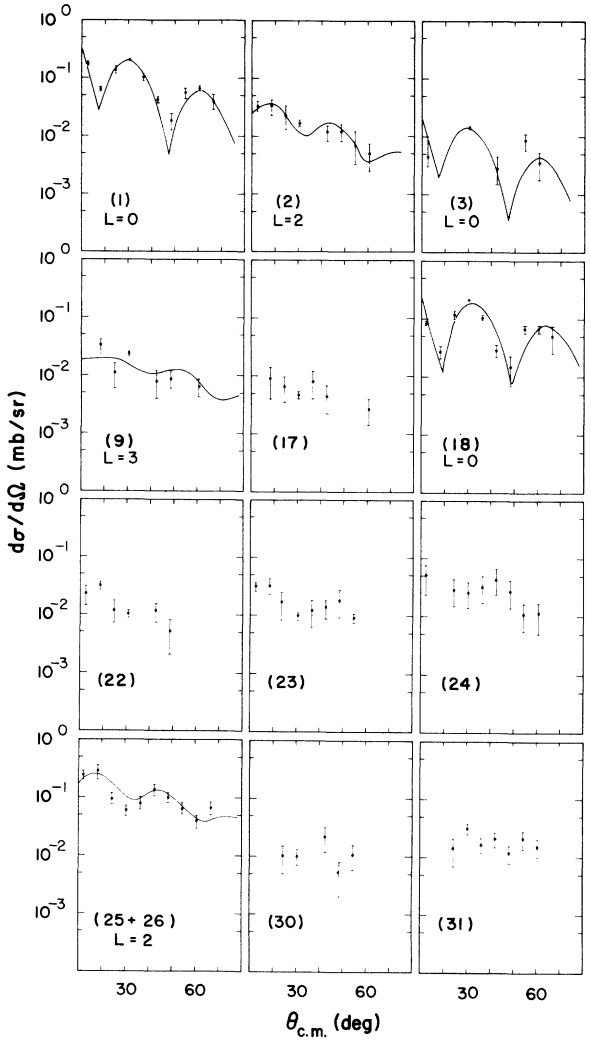

FIG. 6. Cross-section angular distributions for the ^{138}Ce(t, p) reaction. The numbers in parentheses refer to the level numbers of Table V. The solid lines are DWBA fits which have been normalized to the data and represent the L transfer labeled for each case. The DWBA curves are shown only for comparison to the data and do not imply an assignment of L value. All ^{138}Ce(t, p) L value assignments are shown in Table V.

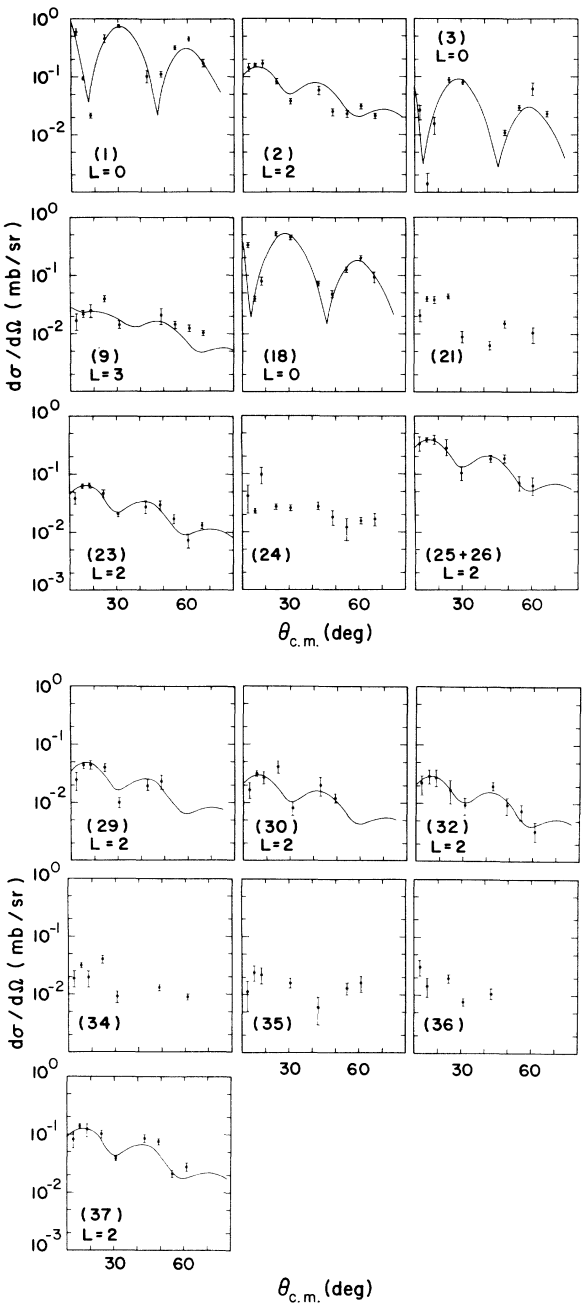

FIG. 7. Cross-section angular distributions for the ^{142}Ce(p,t) reaction. The numbers in parentheses refer to the level numbers of Table V. The solid lines are DWBA fits which have been normalized to the data and represent the L transfer labeled for each case. The DWBA curves are shown only for comparison to the data and do not imply an assignment of L value. All ^{142}Ce(p,t) L value assignments are shown in Table V. It is noted that levels 25 and 26 could be separated at several angles; the level 25 transition is ~4 times stronger than the level 26 transition and the L assignment applies to level 25.

TABLE VI. Optical-model parameters used in DWBA calculations. The form of the imaginary well used for the triton potential was a Woods-Saxon shape, while for the proton well a first derivative of the Woods-Saxon shape was used.

	V (MeV)	r_r (fm)	a_r (fm)	W (MeV)	r_i (fm)	a_i (fm)
Triton potential	166.7	1.16	0.752	15.66	1.498	0.817
^{138}Ce(t,p) proton potential	49.8	1.25	0.65	16.0	1.25	0.47
^{140}Ce(t,p) proton potential	52.2	1.25	0.65	16.0	1.25	0.47
^{142}Ce(p,t) proton potential	52.2	1.25	0.65	16.0	1.25	0.47

ue. This state has been previously identified in the ^{142}Ce(p,t) work of Yagi, Aoki, and Sato.[11] In the (p,t) work of Ball *et al.*[25] on the Nd isotopes, the pairing vibration in the closed-shell nucleus ^{142}Nd was also populated with 60% of the expected strength. The maximum cross sections for selected $L=0$ and $L=2$ transitions are collected in Table VII.

Two additional 0^+ states were observed in ^{140}Ce by both the two-nucleon-stripping and -pickup reactions. The lowest of these states at 1905 keV presumably is a proton excitation, i.e. a state with neutron configurations similar to the ground state but with an orthogonal proton configuration. The neutron-transfer cross section for a pure proton excitation would be quite small, depending upon changes in the proton configurations between the target and residual states. As seen from Table V, the 1905-keV level is excited with ≈7% of the pairing-vibration strength in the (t,p) reaction and with 17% for the (p,t) reaction. These percentages are rather high and suggest some mixing of excited-neutron configurations into this state and perhaps a fraction of the missing pairing-vibrational strength resides here. Recently the level at 3024 keV has been identified as a 0^+ state[12] and Table V indicates that this state has 10% of the ground-state cross section for the (t,p) reaction and 6% for the (p,t) case. The most likely parentage of a 0^+ state at this energy is in the $[2^+(^{140}\text{Ce})\otimes 2^+(^{140}\text{Ce})]_0+2$ phonon quadrupole state. The unperturbed position of such a state would be $2\times E_x(2^+)\sim 3200$ keV rather close to the state under discussion. Again such a state would have only a small overlap with either target ground state and the main source of transition strength probably comes through mixing with the pairing degree of freedom.

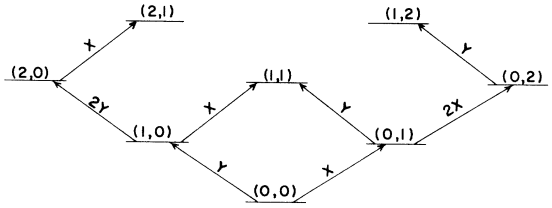

FIG. 8. The harmonic-pairing-vibration model. The arrows represent allowed phonon transitions with intensities being given by the multiples of the basic x or y strengths. The (n_r,n_a) notation signifies the number of phonons in each level, n_r being the number of removal or $B_<^\dagger$ phonons and n_a being the number of addition or $B_>^\dagger$ phonons.

The sum of the transition strengths to these three 0^+ states represents 70% of the expected pairing-vibration strength for the (t,p) reaction and 74% for the (p,t) reaction. The remaining strength could very well be fragmented in other states of the two-phonon type, such as $3^-\otimes 3^-$ etc., at higher excitations.

Larger deviations from the harmonic model are observed further from the closed shell at ^{140}Ce. The 140 → 142 → 144 g.s. cross sections are predicted to be in the ratio 1 : 2, while after DW Q value corrections they are observed to be in the ratio 1 : 1.2. The 136 → 138 → 140 cross sections should also be in the ratio 2 : 1, whereas they are observed to be 1.1 : 1. The energies of the various Ce phonon states are shown in Fig. 9 and it is seen that the harmonic estimate for the three phonon levels

TABLE VII. $L=0$ and $L=2$ maximum cross sections.

Reaction	L value	$(d\sigma/d\omega)^{\max}$ (mb/sr)	c.m. (deg)	Final state E_x (keV)
^{136}Ce$(t,p)^{138}$Ce	0	0.23 [a]	30 [a]	0
^{138}Ce$(t,p)^{140}$Ce	0	0.21	30	0
^{140}Ce$(t,p)^{142}$Ce	0	0.34	30	0
^{142}Ce$(t,p)^{144}$Ce	0	0.41	30	0
^{142}Ce$(p,t)^{140}$Ce	0	0.77	30	0
^{140}Ce$(p,t)^{138}$Ce	0	0.68	24	0
^{138}Ce$(t,p)^{140}$Ce	0	0.21	30	3226
^{142}Ce$(p,t)^{140}$Ce	0	0.53	24	3223
^{140}Ce$(t,p)^{142}$Ce	2	0.60	18	642
^{140}Ce$(p,t)^{138}$Ce	2	0.73	15	790
^{138}Ce$(t,p)^{140}$Ce	2	0.37	18	3551–4119
^{142}Ce$(p,t)^{140}$Ce	2	0.50	18	3654–4188

[a] The measurement was performed at 60°, i.e., at the second maximum of the angular distribution. The 30° number is $\sigma^{138\to 148}(30°)\times[\sigma^{136\to 138}(60°)/\sigma^{138\to 140}(60°)]$.

is about 2 MeV low, i.e., an amount comparable to the one-phonon energy of 2.036 MeV. The situation therefore exhibits pronounced anharmonicities and a more precise treatment of the nuclear structure involved is needed.

Figure 9 demonstrates that the Ce ground state energies can be accounted for reasonably well by the introduction of an empirical two-body interaction between the pairing phonons. There are three such interactions, one between two $B^{\dagger}_{>}$ phonons, one between two $B^{\dagger}_{<}$ phonons, and one between a $B^{\dagger}_{>}$ and a $B^{\dagger}_{<}$ phonon. The first interaction is set equal to the difference between the ^{144}Ce(g.s.) energy and the harmonic prediction and is found to be repulsive. The second interaction, which is also repulsive, is set to be equal to the energy difference for the ^{136}Ce ground state, while the third, attractive interaction is derived from the (1, 1) state of ^{140}Ce. Adding the appropriate number of basic two-body interactions for each 3 or more phonon state gives the results shown by the dotted lines in Fig. 9. The agreement with the

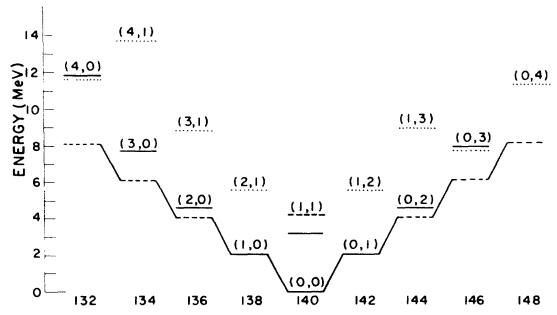

FIG. 9. The energies of the monopole-pairing states in the Ce isotopes. The horizontal solid lines represent the experimental values, the dashed lines represent the harmonic prediction, and the dotted lines represent the anharmonic prediction. The formulas used to give the harmonic-phonon-state energies and the experimental energies are:

$$E(A)_{\mathrm{th}} = 2.036(n_r + n_a)\,,$$

$$E(A)_{\mathrm{exp}} = BE(140) - BE(A) + (7.3145)(A - 140)\,,$$

where $E(A)_{\mathrm{exp}}$ is the experimental energy of the ground state of A relative to the ground state of 140, $BE(A)$ is the binding energy of A, $E(A)_{\mathrm{th}}$ is the theoretical harmonic prediction for the energy of the phonon states of A, and n_r and n_a are the number of $B^{\dagger}_{<}$ and $B^{\dagger}_{>}$ phonons, respectively. These formulas were derived using the experimentally measured Q values for ^{140}Ce(t, p) and ^{138}Ce(t, p). The values used for the binding energies of $^{132, 134, 136, 146}$Ce were taken from the work of J. H. E. Mattauch, W. Thiele, and A. H. Wapstra, Nucl. Phys. 67 1 (1965). The empirically derived two-phonon-interaction matrix elements had the values (1,1) − 0.846, (0,2) +0.538, and (2,0) +0.535. All of the above energies are measured in MeV.

data is seen to be quite good. The anharmonic modifications to the two-nucleon-transfer intensities have so far not been estimated inside this phenomenological approach; however, Sørensen has recently shown that they may be derived to good accuracy from the method of general boson expansions.[26]

D. Pairing-Quadrupole States

The pairing-phonon scheme can be extended to include states with $J \neq 0$. Thus the first 2^+ states in ^{138}Ce and ^{142}Ce can be considered as one-phonon pairing-quadrupole states. The motivation for doing this is twofold. The first excited 2^+ states of $A_0 + 2$ and $A_0 - 2$ nuclei, where A_0 is the closed shell, generally have a large two-particle-transfer cross section. In ^{140}Ce$(t, p)^{142}$Ce, for example, the transition to the 2^+ level at 642 keV is the strongest observed. Secondly, in the closed-shell nuclei there are strong 2^+ levels populated in the region just above the 0^+ pairing vibration. These 2^+ levels can be considered quadrupole-pairing vibrations composed of $B^{\dagger}_{>}B^{\dagger}_{2<}|0\rangle$ or $B^{\dagger}_{2>}B^{\dagger}_{<}|0\rangle$ phonons, where the subscript 2 denotes spin of 2, e.g., $B^{\dagger}_{2>}$ is an operator which creates a one-phonon pairing-quadrupole state for neutrons in orbits above the closed shell.

Using this scheme we would then expect to populate two 2^+ levels in ^{140}Ce at energies of 645 and 790 keV above the 3226 keV 0^+ state (see Fig. 10). The first state at 645 keV above the (1, 1) 0^+ level should be of $B^{\dagger}_{2>}B^{\dagger}_{<}|0\rangle$ character and should be excited via the (t, p) reaction, while the second state at 790 keV above the (1, 1) level should have $B^{\dagger}_{>}B^{\dagger}_{2<}|0\rangle$ character and be seen in the (p, t) reaction. The fact that these states should be separated by only ~150 keV suggests thay they will probably mix. From Table V it is seen that there are at least seven observed 2^+ levels lying 325 to 962 keV above the 3226-keV state which may have significant components of these quadrupole-pairing vibrations. From shell-model considerations one expects the level density of 2^+ states to be higher than that for 0^+ states; therefore, it is not surpris-

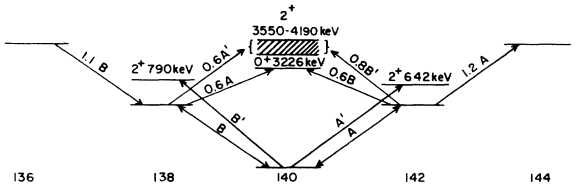

FIG. 10. The observed pairing levels are shown with the relative transition intensities being given by the values written along the arrows.

ing to find a splitting of the 2^+ strength among several levels. If the transition strengths to these levels are summed about 80% of the expected (p, t) cross sections and about 60% of the expected (t, p) intensity is found.

V. CONCLUSIONS

In the present investigation of even Ce nuclei with (t, p) and (p, t) reactions the ^{140}Ce state at 3226 keV has been identified as the two-phonon monopole-pairing vibration possessing about 60% of the expected two-neutron-transfer strength and lying ~850 keV lower than the harmonic prediction. The pairing model was used to interpret the observed ground-state energies and transition strengths to the neighboring even Ce nuclei where anharmonic effects were found to be important. The (p, t) data on the even Nd isotopes[25] also show a fragmentation of the excited 0^+ state strength as one moves away from the shell closure. Comparison of the results around $N=82$ with the Ca(t, p) data[19] and the two-neutron-transfer work around ^{208}Pb [22] indicates that in the single closed-shell region near $N=82$ anharmonic effects are more pronounced and in fact are as important as harmonic terms. For example in the ^{48}Ca and ^{208}Pb cases the (1, 1) state lies close to the predicted energy and receives nearly 100% of the expected harmonic strength as opposed to only 60% for ^{140}Ce and ^{142}Nd. The two-neutron-transfer data near ^{90}Zr and ^{88}Sr indicate even stronger anharmonicities than in the present case.[27] Sørensen[26] has suggested that the fractionation of the (1, 1) strength near $N=50$ can be explained by considering residual terms in the pairing interaction and mixing with various two-phonon surface vibrations such as $(3^- \times 3^-)^{J=0}$ and $(2^+ \times 2^+)^{J=0}$. A similar mechanism has been suggested above for the observed anharmonicites in the present case.

The situation with regard to the quadrupole-pairing vibrations is similar to the monopole case. Larger fractionation and loss of two-neutron-transfer cross section are observed in the singly-closed-shell cases than are observed for doubly magic ^{48}Ca and ^{208}Pb. Higher-order multipole-pairing vibration states were not observed in ^{140}Ce in spite of the fact that strong (t, p) transitions were observed above the first 2^+ state in the ^{140}Ce(t, p) reaction. Thus the two-phonon hexadecapole strength, for example, is probably entirely fragmented in ^{140}Ce.

In conclusion the present experiment has confirmed the identification of the principal pairing monopole and quadrupole states of the even Ce isotopes and measured their deviation in strength and energy from a harmonic description. Although the anharmonic effects are large, these states still retain most of their pairing collectivity and provide a useful addition to the known collective states of Ce.

ACKNOWLEDGMENTS

It is a pleasure to acknowledge the cooperation of the staff of the Los Alamos Van de Graaff facility and the scanning group of the Physics Division. Special thanks are due S. D. Orbesen for his help in taking the data and to R. Leonard of Florida State University who produced the isotope-separator targets. One of us (T.J.M.) wishes to acknowledge the Associated Western Universities, Inc., for financial support.

---

*Work performed under the auspices of the U. S. Atomic Energy Commission.

†Associated Western Universities, Inc., fellow from Florida State University.

[1]A. Bohr, in *Nuclear Structure* (International Atomic Energy Agency, Vienna, Austria, 1968), p. 179.

[2]O. Nathan, in *Nuclear Structure* (see Ref. 1), p. 191.

[3]D. R. Bes and R. A. Broglia, Nucl. Phys. 80, 289 (1966).

[4]H. W. Baer, J. J. Reidy, and M. L. Wiedenbeck, Nucl. Phys. A113, 33 (1968).

[5]J. T. Larsen, W. L. Talbert, Jr., and J. R. McConnell, Phys. Rev. C 3, 1372 (1971).

[6]G. M. Julian and T. E. Fessler, Phys. Rev. C 3, 751 (1971).

[7]R. H. Fulmer, A. L. McCarthy, and B. L. Cohen, Phys. Rev. 128, 1302 (1962).

[8]C. A. Wiedner, A. Heusler, J. Solf, and J. P. Wurm, Nucl. Phys. A103, 433 (1967).

[9]R. A. Brown and R. L. Mlekodaj, Phys. Rev. C 3, 954 (1971).

[10]W. P. Jones, L. W. Borgman, K. T. Hecht, J. Bardwick, and W. C. Parkinson, Phys. Rev. C 4, 580 (1971).

[11]K. Yagi, Y. Aoki, and K. Sato, Nucl. Phys. A149, 45 (1970).

[12]J. D. Sherman, B. G. Harvey, D. L. Hendrie, and M. S. Fisman, private communication.

[13]F. G. Perey, Phys. Rev. 131, 745 (1965).

[14]E. R. Flynn, D. D. Armstrong, J. G. Beery, and A. G. Blair, Phys. Rev. 182, 1113 (1969).

[15]S. Raman, Nucl. Data B2 (No. 1), 112 (1967).

[16]P. A. Seeger, private communication.

[17]B. F. Bayman and A. Kallio, Phys. Rev. 156, 1121 (1967).

[18]E. R. Flynn and O. Hansen, Phys. Letters 31B, 135 (1970).

[19]O. Hansen and O. Nathan, Nucl. Phys. 42, 197 (1963).

[20]J. Bjerregaard, O. Hansen, O. Nathan, R. Chapman,

S. Hinds, and R. Middleton, Nucl. Phys. A103, 33 (1967).
[21]R. Broglia, P. Federman, O. Hansen, K. Hehl, and C. Riedel, Nucl. Phys. A106, 421 (1968).
[22]R. Broglia and C. Riedel, Nucl. Phys. A92, 145 (1967).
[23]E. R. Flynn, R. Broglia, S. Landowne, B. Nilsson, and V. Paar, Nucl. Phys. (to be published).
[24]O. Hansen, in *Proceedings of the International Conference on Properties of Nuclear States, Montréal, Canada, 1969*, edited by M. Harvey *et al.* (Presses de l'Université de Montréal, Montréal, Canada, 1969), p. 421.
[25]J. B. Ball, R. L. Auble, J. Rapaport, and C. B. Fulmer, Phys. Letters 30B, 533 (1969).
[26]B. Sørensen, Nucl. Phys. (to be published).
[27]J. Ball, R. Auble, and P. Roos, Phys. Rev. C 4, 196 (1971).

PHYSICAL REVIEW C VOLUME 6, NUMBER 5 NOVEMBER 1972

Elastic Scattering of ^{16}O by ^{56}Fe, $^{70,74}Ge$, and ^{90}Zr†

A. W. Obst, D. L. McShan, and R. H. Davis
Department of Physics, The Florida State University, Tallahassee, Florida 32306
(Received 2 August 1972)

The elastic scattering of ^{16}O by ^{56}Fe, ^{70}Ge, ^{74}Ge, and ^{90}Zr has been studied in the vicinity of the Coulomb barrier for the purpose of extracting optical-model parameters and barrier heights. Angular distributions were measured from 30° to 170° in the lab in 10° steps and in the bombarding energy range from 30 to 60 MeV in 2-MeV steps. No discrete ambiguities in the real potentials were found, probably due to the large imaginary potentials. Barrier heights determined with the optical-model parameters were found to be consistent with Greiner's calculated barrier heights and 10–20% lower than the ordinary Coulomb barrier $Z_1Z_2e^2/1.35(A_1^{1/3}+A_2^{1/3})$.

I. INTRODUCTION

Credible predictions of the barrier height, the energy at which two nuclear masses just touch, are important to the design of future experiments with very heavy ions. In the adiabatic approximation model used by Beringer,[1] the two colliding masses become oblate with respect to a common axis, with the result that the interaction barrier is significantly raised above that for two spheres. Greiner[2] and others[3,4] have predicted barriers by solving the time-dependent collision problem, in which the collision time and the characteristic oscillation periods of the individual nuclei are related. For oscillation periods longer than the collision time, the nuclei do not have time to align themselves preferentially and the barrier is lowered. Oscillation periods shorter than the collision time are more difficult to excite, but once excited can also reduce the barrier by the periodic extension of the nuclei towards one another. It is, furthermore, not clear to what extent the nuclear diffuseness affects the above considerations.[3]

The two most straightforward methods of measuring the height of the barrier are optical-model analysis of elastic scattering and the onset of reactions. Systematic data of either type are scarce for heavy ions.[5] A third possible means of establishing the barrier is in the interference minima in inelastic heavy-ion scattering.[6] However, until these can be sufficiently well correlated with theory, a precise determination of the barrier this way is difficult.

In the present work optical-model analysis of elastic scattering was used to find barrier heights for ^{16}O on several medium-weight nuclei from ^{40}Ca to ^{120}Sn. These are compared with the classical values and also with the predictions of the dynamic models. The results for Ni are compared to available (^{16}O, xn) and (^{16}O, xp) measurements.

II. EXPERIMENTAL METHOD

The Florida State University super FN tandem Van de Graaff was used to produce a beam of 30- to 60-MeV ^{16}O ions of charge states 5 or 6. Fifteen point angular distributions were measured in 2-MeV steps using 15 Si surface-barrier detectors mounted in a ring at 10° intervals from 30 to 170° in the lab. The over-all energy resolution was about 300–500 keV, as seen in Fig. 1.

Also seen in Fig. 1 are the first-excited-state 2^+ groups in ^{56}Fe (0.845 MeV), ^{70}Ge (1.04 MeV), ^{74}Ge (0.596 MeV), and ^{90}Zr (2.18 MeV); the second 2^+ state groups in ^{74}Ge (1.20 MeV); the third 2^+ state in ^{90}Zr (3.84 MeV); and the first 3^- state group in ^{90}Zr (2.74 MeV). At the forward angles these excited-state groups are barely discernible